Tempering of Martensite and Subsequent Redistribution of Cr, Mn, Ni, Mo, and Si Between Cementite and Martensite Studied by Magnetic Measurements

JAVAD MOLA, GUOQING LUAN, DAVID BROCHNOW, OLENA VOLKOVA, and JUN WU

Tempering reactions in ternary Fe-2M-0.7C steels (M = Cr, Ni, Mn, Mo, and Si) were studied by correlative dilatometry and magnetic measurements at room temperature. Magnetic measurements were conducted after tempering at progressively higher temperatures. Based on the magnitude of demagnetization in the temperature range associated with the tempering stage I contraction, Mn- and Si-added steels formed the largest and smallest fractions of transition carbides, respectively. Estimation of the magnetization of paraequilibrium cementite indicated that Cr, Mn, and Mo reduced the magnetization while Ni increased it. In the presence of Si, the decomposition of retained austenite and cementite formation were shifted to higher temperatures. At temperatures above approximately 723 K (450 °C), the enrichment of cementite with Mn and Cr significantly reduced the total magnetization. In the Mo-added steel, on the other hand, the magnetization slightly increased implying the formation of ferromagnetic Mo-rich carbides. For the Ni- and Si-added steels, the magnetization remained almost constant indicating minimal redistribution of Ni and Si subsequent to the formation of cementite. The possibility of analyzing the latter redistribution is one of the main advantages of sequential tempering and magnetic measurements at room temperature compared to *in situ* thermomagnetic measurements.

DOI: 10.1007/s11661-017-4374-5

I. INTRODUCTION

THERMAL agitation of martensite leads to a number of aging and tempering reactions. Aging reactions, collectively termed the zeroth stage of tempering, include pre-precipitation phenomena such as the redistribution of solute carbon atoms to martensite imperfections such as dislocations, boundaries, sub-boundaries, and interfaces with retained austenite. The occurrence of these processes has been confirmed by atom probe tomography (APT) investigations.[1–3] Another structural change which can occur near room temperature (RT) is the formation of a modulated structure consisting of alternating carbon-rich and essentially carbon-free regions.[4]

The tempering stage I involves the formation of transition carbides with hexagonal (ε-carbides)[5] or orthorhombic (η-carbides)[6] crystal symmetries, the former being reported more often. In the tempering stage II, retained austenite in carbon and low-alloy steels decomposes by transformation to bainite.[7] The tempering stage III is characterized by the gradual dissolution of transition carbides and the precipitation of orthorhombic cementite (θ) or monoclinic Hägg (χ) carbides.[8] The tempering stage IV, specific to steels containing carbide-forming alloying elements, involves the formation of alloy carbides.[9]

Dilatometry analysis of length changes associated with tempering reactions is a quick method of studying tempering reactions.[10–15] Due to the difficulty of obtaining martensitic steels without retained austenite under practical conditions, the overlap of the expansion due to the austenite decomposition (stage II) and the contractions associated with the tempering stages I and III might interfere with the interpretation of dilatometry results for carbon and low-alloy steels containing retained austenite.[16] In the present study, tempering

JAVAD MOLA, GUOQING LUAN, DAVID BROCHNOW, and OLENA VOLKOVA are with the Institute of Iron and Steel Technology, Technische Universität Bergakademie Freiberg, Leipziger St. 34, 09599 Freiberg, Germany. Contact e-mail: mola@iest.tu-freiberg.de JUN WU is with The State Key Laboratory of Refractories and Metallurgy, Faculty of Materials and Metallurgy, Wuhan University of Science and Technology, Wuhan, 430081, P.R. China.
Manuscript submitted March 6, 2017.
Article published online October 13, 2017

reactions in ternary low-alloy steels are studied by correlative dilatometry and magnetic measurements at RT. The latter technique is particularly sensitive to retained austenite decomposition and partitioning of alloying elements between carbides and martensite. Compared to *in situ* thermomagnetic measurements in which magnetization is measured during continuous heating,[17,18] the present method of tempering at progressively higher temperatures and magnetic measurements at RT offers the following advantages. Measurements at RT as the reference temperature eliminate the need to know the temperature dependence of magnetization for constituents. Furthermore, whereas magnetic and thermal systems in thermomagnetic measurements are integrated and their coupling might limit the choice of the systems employed, the introduced method can be applied using dedicated magnetic measurement and thermal treatment systems. Even if the same magnetic system is used for both measurements, the higher magnetization levels at RT will lead to an enhanced quality of data in the case of *ex-situ* measurements at RT. As a result, the present magnetic method is even applicable to the study of the redistribution of alloying elements between martensite and cementite.

II. EXPERIMENTAL METHODS

Ingots of Fe-M-C ternary steels (M denoting Cr, Mn, Ni, Si, and Mo) and a reference Fe-C binary steel with the chemical compositions given in Table I were produced in a cold-crucible induction melting facility. Ingots were homogenization annealed at 1473 K (1200 °C) for 2 hours. Final hardening was done by austenitization at 1273 K (1000 °C) for 10 minutes followed by quenching in a mixture of brine (10 pct NaCl) and ice for 3 seconds and subsequently transferred to a tank of liquid nitrogen at 77 K (−196 °C). A Zeiss AXIO Scope.A1 light optical microscope was used to confirm the absence of pearlite in hardened specimens. Magnetic measurements were done using a Metis MSAT device equipped with a Lakeshore 480 fluxmeter (magnetic field intensity > 3.77 kOe). Three specimens of each steel with an approximate mass of 3 g and an approximate thickness of 3.5 mm were used for magnetic measurements. The change in the magnetization of specimens by tempering at progressively higher temperatures in the range of 323 K to 923 K (50 °C to 650 °C) with increments of nearly 50 K was determined by magnetic measurements at RT. Tempering was done in a muffle furnace and holding time prior to water quenching was 5 minutes. Temperature during tempering was monitored by means of a thermocouple attached to a reference specimen. Temperature equalization of specimens with the preheated furnace took approximately 2 minutes. Due to the small thickness of specimens, through-thickness temperature inhomogeneities were neglected. Dimensional changes associated with tempering reactions were studied during continuous heating of as-quenched specimens in a Bähr-DIL805 dilatometer. Dilatometry was also used to determine the martensite start temperatures. The holding time at the austenitization temperatures of 1273 K to 1323 K (1000 °C to 1050 °C) was 30 seconds. Cooling rates to RT were in the range 50 to 80 K/s. Dilatometry specimens had a dimension of $3.5 \times 3.5 \times 10$ mm^3. Thermo-Calc with the TCFE8 database was used for the thermodynamic equilibrium calculations.

III. RESULTS AND DISCUSSION

A. *Hardened State*

Figure 1 shows relative length changes during cooling of alloys from the austenite range. The martensite start temperatures marked in Figure 1 were determined using the strain offset method at an offset expansion corresponding to 5 vol pct α' martensite formation.[19] Martensite start temperatures are in the range of 495 K to 526 K (222 °C to 253 °C) confirming that high martensite fractions could be obtained by the applied hardening treatment. Metallographic examination results confirmed the absence of pearlite in all hardened ternary steels except the 2Ni steel whose microstructure contained less than 1 vol pct pearlite which was neglected.

In order to quantify martensite and retained austenite fractions in hardened specimens, magnetic measurements were performed at RT. Measured mass magnetizations of hardened specimens are given in Table II. The equipment is capable of converting the measured magnetizations into ferrite/martensite fractions by dividing them by the expected magnetization of ferrite/martensite. The expected magnetization is calculated by an internal calibration which takes into account

Table I. Chemical Compositions in Mass-Pct

Alloy ID	C	Cr	Mn	Si	Ni	Mo	Fe
FeC	0.69	0.025	0.051	<0.005	0.014	<0.005	bal.
2Cr	0.68	**2.10**	0.050	<0.005	<0.005	0.007	bal.
2Mn	0.70	0.030	**2.37**	<0.005	<0.005	<0.005	bal.
2Si	0.69	0.019	0.052	**2.00**	0.015	<0.005	bal.
2Ni	0.71	0.018	0.048	<0.005	**2.04**	<0.005	bal.
2Mo	0.71	0.019	0.055	0.011	0.013	**1.95**	bal.

The main substitutional alloying element is highlighted in bold.

the effect of alloying elements on the magnetization of pure iron. Nevertheless, the observation of a ferromagnetic phase fraction of less than 100 vol pct in the case of pure iron indicated the inaccuracy of the preset values. Therefore, to exclude errors arising from an incorrect preset magnetization for pure iron and inaccurate representation of the effect of alloying elements on the magnetization of pure iron, the raw magnetizations were used for the quantification of retained austenite. The additional advantage of using magnetizations is the possibility of incorporating ferromagnetic phases other than ferrite/martensite, *e.g.*, cementite. The phase fractions in the hardened specimens were quantified by applying the rule of mixtures in the following form to the measured magnetizations.

$$\sigma_{RT} = \sigma_{RT,\alpha'} \times f_{\alpha'} + \sigma_{RT,\gamma} \times f_{\gamma}. \quad [1]$$

In Eq. [1], σ_{RT} denotes the measured magnetization at RT; $\sigma_{RT,\alpha'}$ and $\sigma_{RT,\gamma}$ refer to the magnetizations of martensite and austenite at RT, respectively; and $f_{\alpha'}$ and f_{γ} denote the phase fractions of martensite and austenite, respectively. Due to the paramagnetism of austenite, $\sigma_{RT,\gamma}$ was replaced with zero. Since $f_{\gamma} = 1 - f_{\alpha'}$, the fraction of austenite can be calculated using the following equation:

$$f_{\gamma} = 1 - \frac{\sigma_{RT}}{\sigma_{RT,\alpha'}}. \quad [2]$$

According to Eq. [2], the knowledge of $\sigma_{RT,\alpha'}$ is essential to the quantification of retained austenite. In order to estimate $\sigma_{RT,\alpha'}$, the influence of alloying elements on the RT magnetization of pure iron, $\sigma_{RT,Fe}$, was estimated from linear relationships of the form:

$$\sigma_{RT,\alpha'} = \sigma_{RT,Fe} + X_{AE} \times C_{AE}, \quad [3]$$

where X_{AE} is a coefficient whose sign and magnitude indicate the efficiency of each mass-pct of the alloying element AE in changing the magnetization of pure iron, and C_{AE} indicates the concentration of AE in mass-pct. The X_{AE} values listed in Table III were obtained from literature data reporting magnetization values for binary steels. The magnetization of pure iron was determined to be 213.5 emu/g which is almost identical to the reported RT value at an external field of 4 kOe.[20] The $\sigma_{RT,\alpha'}$ values calculated by means of Eq. [3], the σ_{RT} values, and the retained austenite contents based on Eq. [2] are given in Table II. Retained austenite contents of all specimens lie in the range of 4.8 to 6 vol pct.

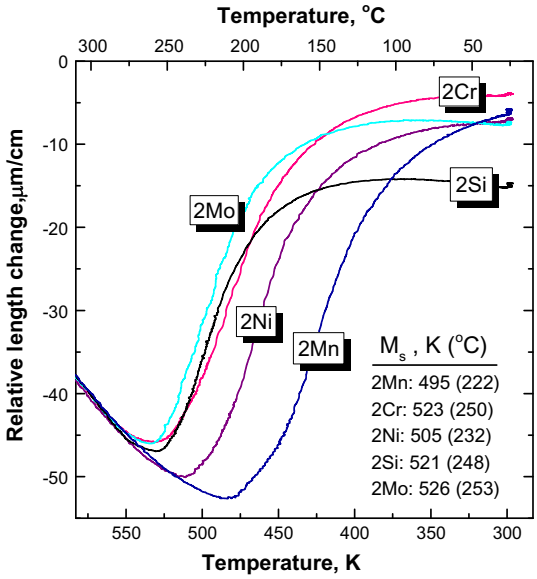

Fig. 1—Relative length changes during cooling of steels from austenite range and martensite start temperatures determined by the strain offset method. Austenitization temperatures and cooling rates from austenitization temperatures were 1273 K to 1323 K (1000 °C to 1050 °C) and 50 to 80 K/s, respectively.

B. *Dilatometry*

Coefficients of thermal expansion (CTE_a) obtained from the first derivative of relative length changes during continuous heating of hardened specimens at a rate of 0.2 K/s are shown in Figure 2. Due to the different nature of experiments in dilatometry and magnetic measurements, it is difficult to define a heating rate in dilatometry which precisely corresponds to the isothermal tempering treatments in magnetic measurements. In order to choose an appropriate heating rate in dilatometry cycles, factors such as heating rate to the isothermal tempering temperature, holding time at each temperature, and the interval between tempering temperatures should be taken into account. The basis for the selection of a heating rate of 0.2 K/s in dilatometry experiments was our preliminary experiments with martensitic stainless steels. The absence of the tempering stage II in stainless steels allows to identify the onset of cementite formation by dilatometry.[26] In magnetic measurements, on the other hand, the onset of cementite formation can be readily identified based on the associated reduction in magnetization.[27] By applying

Table II. Measured Magnetizations (σ_{RT}) and Retained Austenite Contents in Hardened Steels Calculated based on Expected Magnetizations in the Fully Martensitic State ($\sigma_{RT,\alpha'}$)

Alloy ID	σ_{RT}, emu/g	$\sigma_{RT,\alpha'}$, emu/g	f_{γ}, Vol Pct
2Cr	198.5	209.0	5.0
2Mn	198.0	210.7	6.0
2Si	198.0	209.5	5.5
2Ni	204.2	214.4	4.8
2Mo	198.4	209.6	5.4

Table III. Changes in the Magnetization of Pure Iron by Alloying Elements

Alloying Element (AE)	X_{AE}, emu/g per 1 Mass-Pct AE	Reference
Cr	−2.12	21
Mn	−1.18	22
Si	−2.00	23
Ni	+0.45	24
Mo	−1.98	25

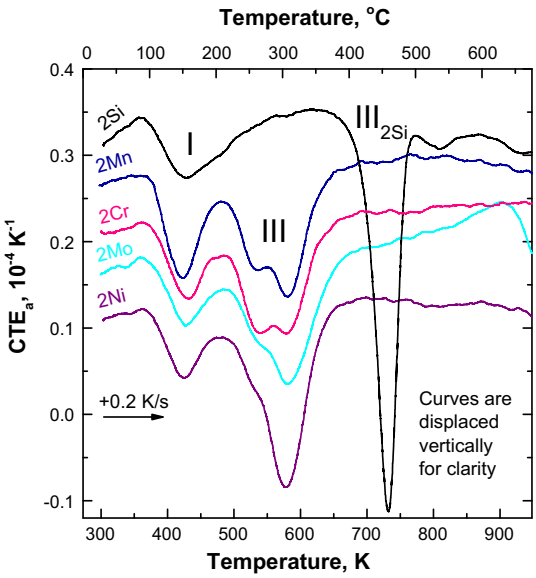

Fig. 2—CTE_a values during continuous heating of hardened steels. Curves except that for the 2Ni steel are displaced upwards in multiple increments of 0.05×10^{-4} K^{-1}.

various dilatometry heating rates to martensitic stainless steels, the range of heating rates corresponding to the isothermal tempering conditions similar to those applied in the present work was found to be 0.1 to 0.2 K/s. In CTE_a curves during continuous heating, reactions associated with contraction under isothermal conditions decrease the CTE_a. Reactions associated with expansion under isothermal conditions, on the other hand, increase the CTE_a. Accordingly, the CTE_a reduction marked I in Figure 2 corresponds to the volume contraction accompanied by the tempering stage I, which is often attributed to the formation of transition carbides.[10,12,14,26] The second noticeable decrease in the CTE_a values, denoted III in Figure 2, marks the formation of cementite. For all steels except the 2Si, the temperature range associated with the tempering stage III is almost identical. Delayed formation of cementite in the 2Si steel is in agreement with the well-known effect of Si on the formation of paraequilibrium cementite.[28]

The CTE_a curves show additional fluctuations, especially during the tempering stage III contraction. These fluctuations are most likely due to the expansion associated with the decomposition of retained austenite.[10] Due to small volume fractions of retained austenite, precise identification of the temperature range associated with the decomposition of retained austenite is not straightforward. Figure 2 also indicates that with the exception of the 2Mo steel, CTE_a values subsequent to the tempering stage III remain almost constant. For the 2Mo steel, CTE_a values gradually increase at temperatures above approximately 723 K (450 °C) implying the occurrence of other types of carbides induced by the Mo addition.

C. *Sequential Tempering and Magnetic Measurements*

1. *Tempering stages I to III*

Figure 3(a) shows the variation of mass magnetizations ($\sigma_{\text{-RT}}$) as a function of the prior tempering temperature. The RT values are equal to those used for the quantification of retained austenite contents. Subsequent changes in magnetization could be attributed to the occurrence of tempering reactions. These changes are smallest for the Fe-C steel with a mainly pearlitic microstructure. In order to obtain the values in Figure 3(a), measured magnetizations were divided by the mass of specimens prior to sequential tempering and magnetic measurements. However, possible oxidation during tempering of specimens decreases the $\sigma_{\text{-RT}}$ values. Additional magnetic measurements using the Fe-C steel with intermediate polishing between each tempering and magnetic measurement step indicated the constancy of magnetization above 673 K (400 °C). Accordingly, the linear demagnetization of the Fe-C steel at temperatures above 673 K (400 °C) is best explained by the occurrence of oxidation and can be used to exclude the effect of surface oxidation on the magnetization of ternary steels. The correction was done by raising the measured magnetizations of the ternary steels at temperatures above 673 K (400 °C) by increments of $0.0076 \times (T\text{-}673)$ emu/g, where T is the tempering temperature in Kelvin. This offset was obtained by making a linear fit to the magnetization values of the Fe-C steel at temperatures above 673 K (400 °C) and corrects the decreasing magnetization of the Fe-C steel to an almost constant level.

The corrected magnetizations are shown in Figures 3(b through f). The approximate temperature range for the tempering stage II was determined based on the associated increase in the magnetization level. The temperature ranges associated with the tempering stages I and III, on the other hand, were marked based on a correlation with the dilatometry results. Due to the lower magnetization of transition carbides compared to martensite,[29] a demagnetization is expected upon the formation of such carbides in the tempering stage I. The demagnetization during the stage I tempering depends on the chemical composition. The largest and smallest demagnetizations during the stage I tempering occurred in the case of the 2Mn and 2Si steels, respectively. The magnitude of stage I demagnetization could have been influenced by the increase in magnetization due to the decomposition of retained austenite. In other words, retained austenite decomposition at low temperatures could mask some of the demagnetization due to the transition carbides formation. Due to the retarded

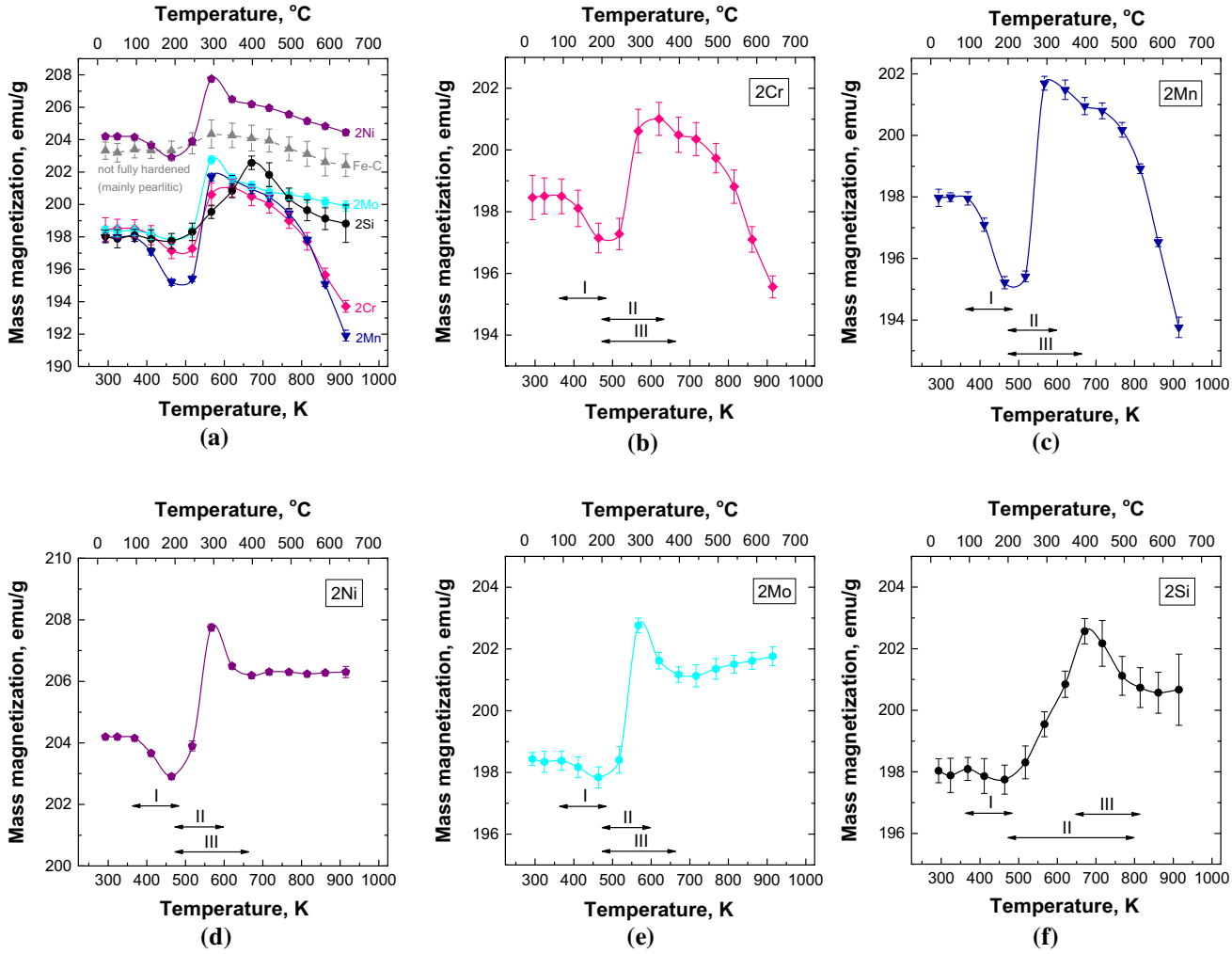

Fig. 3—(*a*) Changes in magnetization upon tempering at progressively higher temperatures; (*b* to *f*) changes in magnetization after correction for the effect of surface oxidation. Tempering stages I to III are marked based on a correlation with dilatometry results.

decomposition of retained austenite in the 2Si steel, the absence of noticeable demagnetization during its stage I contraction cannot be attributed to the concurrent decomposition of retained austenite. Therefore, transition carbides formation is likely suppressed in the 2Si steel. On this basis, the observed stage I contraction could be attributed to such phenomena as the segregation of carbon atoms to martensite defects, a process also associated with volume contraction.[11] Stage I contraction without noticeable demagnetization is also a characteristic of high-interstitial stainless steels.[27] The constancy of magnetization during stage I contraction confirms the negligible effect of solute C on the magnetization of martensite.

At temperatures above approximately 473 K (200 °C), the tempering stages II and III occur in parallel with opposing effects on the total magnetization. For all steels except the 2Si steel, the increase in magnetization is interrupted at 573 K to 623 K (300 °C to 350 °C), suggesting the end of stage II. The rapid demagnetization of the 2Ni and 2Mo steels between 573 K (300 °C) and 623 K (350 °C) suggests the ongoing formation of cementite. In the 2Si steel, the formation of cementite and the decomposition of retained austenite both occurred at higher temperatures than the other steels. Although the increase in the magnetization of the 2Si steel is interrupted at 673 K (400 °C), the decomposition of retained austenite may continue into the cementite formation range. However, the associated magnetizing effect of retained austenite decomposition can be counteracted by the formation of a high cementite fraction over a narrow temperature range. This explains the demagnetization occurring between 673 K (400 °C) and 823 K (550 °C).

Cementite formation in martensitic steels occurs under paraequilibrium conditions without partitioning of substitutional alloying elements. Since the stages II and III in all steels except the 2Si steel are complete at 673 K (400 °C) and this temperature is low enough to ensure negligible substitutional partitioning, the magnetization values at 673 K (400 °C) were used to estimate the magnetization of cementite ($\sigma_{RT,\theta}$). Due to the continued formation of cementite in the 2Si steel at temperatures up to 823 K (550 °C), the 2Si steel was

excluded from calculations. In order to obtain $\sigma_{RT,\theta}$ values, the rule of mixtures was applied in the following form:

$$\sigma_{RT}^{T673} = \sigma_{RT,\alpha'} \times f_{\alpha'}^{T673} + \sigma_{RT,\theta} \times f_{\theta}^{T673}, \quad [4]$$

where σ_{RT}^{T673} denotes the magnetization at RT after tempering at 673 K (400 °C); $\sigma_{RT,\alpha'}$ represents the magnetization of martensite; and $f_{\alpha'}^{T673}$ and f_{θ}^{T673} denote the phase fractions of martensite and cementite after tempering at 673 K (400 °C), respectively. Due to the completion of the tempering stage III, transition carbides do not appear in Eq. [4]. Since the substitutional content of martensite does not change after tempering at 673 K (400 °C), $\sigma_{RT,\alpha'}$ values in Eq. [4] were taken from Table II. The fractions of martensite and cementite after tempering at 673 K (400 °C) were then determined by neglecting the solute C and the C tied up in dislocations[7,30–32] and assuming that all C has precipitated as cementite. Furthermore, this temperature is too low for the formation of alloy carbides.[9,33] Magnetizations after tempering at 673 K (400 °C), cementite fractions, and calculated $\sigma_{RT,\theta}$ values are listed in Table IV. Using an annealed Fe-1.42 mass-pct C binary steel with a microstructure consisting of ferrite and cementite, the magnetization of pure Fe_3C was estimated to be 130 emu/g, close to the reported values for cementite.[29] The values in Table IV, which also lie in the vicinity of 130 emu/g, reflect the influence of substitutional alloying elements in amounts equal to the nominal composition on the magnetization of cementite. The results indicate that Mn, Cr, and Mo decrease the magnetization of cementite whereas Ni increases it. These results are in qualitative agreement with the reported effects of these elements on the magnetization or the Curie temperature of cementite.[34–36]

2. *Elemental redistribution between martensite and cementite*

If the tempering temperature is high enough to enable the diffusion of substitutional alloying elements in both martensite and cementite, they may redistribute between phases. The redistribution of alloying elements is governed by their influence on the free energies of martensite and cementite. The thermodynamic calculations in Table V give the equilibrium partitioning factor, namely the equilibrium concentration of alloying elements in cementite divided by their equilibrium concentration in martensite at 923 K (650 °C). Partitioning factors are higher than unity for Cr, Mn, and Mo indicating their preference to partition into cementite. A partitioning factor of 0.3 for Ni, on the other hand, indicates its preference to partition out of cementite. The partitioning factor of zero for Si indicates its insolubility in cementite.

Table IV. Measured Magnetizations after Tempering at 673 K (400 °C) (σ_{RT}^{T673}), Cementite Contents, and Calculated Magnetizations for Paraequilibrium Cementite ($\sigma_{RT,\theta}$) based on Eq. [4]

Alloy ID	σ_{RT}^{T673}, emu/g	f_θ, Vol Pct	$\sigma_{RT,\theta}$, emu/g
2Cr	200.5	9.9	122
2Mn	200.9	10.2	115
2Ni	206.2	10.3	135
2Mo	201.2	10.3	128

The elemental redistribution subsequent to the formation of paraequilibrium cementite in martensite influences the magnetization of both phases. For instance, in many studies involving the use of APT, Mn and Cr have been shown to partition into cementite.[31,32,37] An increase in the solute Mn and Cr contents of cementite will in turn reduce the magnetization of cementite while increasing that of the martensitic matrix. The net effect of redistribution on the total magnetization depends on the phase fractions and the influence of alloying elements on the magnetization of phases.

The calculations summarized in Figure 4 aim to demonstrate how the partitioning of Cr between martensite and cementite in the 2Cr steel can change the total magnetization with respect to the value at 673 K (400 °C), namely the value before any conceivable redistribution can occur. The calculations show how the Cr content of martensite, the magnetizations of martensite and cementite, and the total magnetization are varied as the Cr concentration of cementite is raised. It is assumed that the Cr distribution in each phase is uniform. The increase in the magnetization of martensite was calculated based on the coefficient X_{Cr} in Table III. The decrease in the magnetization of cementite, on the other hand, was estimated based on the data in Reference 36 which imply that the presence of approximately 12 mass-pct Cr in cementite makes it paramagnetic at RT. The magnetization of cementite was assumed to decrease linearly with Cr at a rate of 10.7 emu/g per mass-pct Cr. According to Figure 4, the total magnetization decreases to 190.6 emu/g as the average Cr content of cementite increases to 12 mass-pct.

In Figures 3(b, c), the pronounced decrease in the magnetization of 2Cr and 2Mn steels at temperatures above 723 K (450 °C) could be attributed to the partitioning of these elements into cementite. The partitioning of alloying elements between cementite and martensite in low-alloy steels has been demonstrated for specimens tempered 10 hours at 673 K (400 °C)[31] or 2 hours at 723 K (450 °C),[32] and to smaller extent after 5 minutes at 723 K (450 °C).[37] The critical amount of solute atom in cementite needed to turn it paramagnetic at RT has been reported to be somewhere between 8 mass-pct[38] and 12 mass-pct[36,39] for Cr and 8 mass-pct for Mn.[35,39] Although the smaller rate of demagnetization for the 2Cr steel might be related to the higher efficiency of Mn in demagnetizing cementite, the possibility of partial replacement of cementite with paramagnetic Cr-rich carbides cannot be excluded. The latter process would lead to the Cr-depletion of undissolved cementite thereby increasing its magnetization and decelerating the total rate of demagnetization.

The magnetization of the 2Ni steel remains almost constant at temperatures above 673 K (400 °C). This is in agreement with experimental results[31,32] and

Table V. Equilibrium Partitioning Factors for Alloying Elements at 923 K (650 °C) as Calculated by Thermo-Calc

Alloying Element (AE)	Cr	Mn	Mo	Ni	Si
$AE_\theta/AE_{\alpha'}$	51.0	13.6	7.6	0.3	0

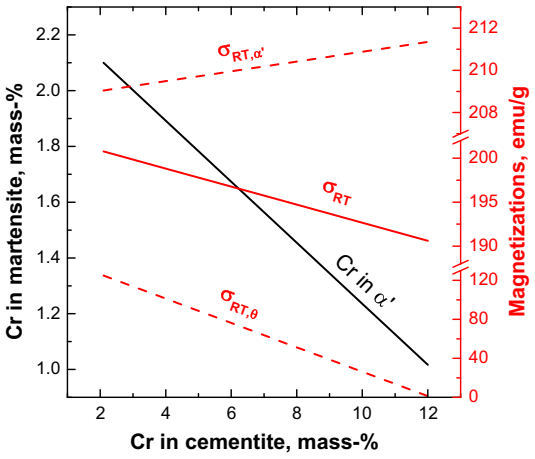

Fig. 4—Hypothetical calculations demonstrating how the Cr enrichment of paraequilibrium cementite in the 2Cr steel influences the Cr content of martensite. Concurrent changes in the RT magnetization of martensite, cementite, and total magnetization are also shown.

thermodynamic calculations in Table V indicating the weak tendency of Ni to partition into martensite. Mo, on the other hand, has been reported to partition into cementite but to a smaller extent than Cr and Mn.[32] Furthermore, because of the weaker efficiency of Mo in depressing the Curie temperature of cementite compared to Cr and Mn,[34] the demagnetization upon Mo partitioning into cementite is expected to be smaller. In practice, the magnetization of the 2Mo steel slightly increases at temperatures above 673 K (400 °C). Supported by the volume expansion at temperatures above 723 K (450 °C) (Figure 2), Mo might have favored the formation of Mo-rich precipitates of types M_2C and M_6C.[9,40] The secondary hardening effect of Mo in carbon steels is explained by the occurrence of Mo-rich M_2C carbides.[9] The absence of demagnetization in the 2Mo steel implies the formation of ferromagnetic Mo-rich carbides which inhibit the partitioning of Mo into existing cementite precipitates.

The growth of cementite in Si-added steels is well known to be associated with the escape of Si into the surrounding ferritic matrix.[41] Accordingly, cementite in the 2Si steel is expected to contain a low Si content as it forms. Therefore, due to occurrence of Si redistribution between cementite and martensite during its formation at temperatures below 823 K (550 °C), the magnetization of the 2Si steel remains almost constant at higher temperatures (Figure 3(f)).

The Curie temperature of cementite is usually lower than its formation temperature and much lower than temperatures where elemental redistribution between cementite and martensite is enabled. This limits the applicability of *in situ* thermomagnetic measurements to the analysis of elemental redistribution because the magnetization of cementite is zero as it forms during thermomagnetic measurements and remains zero at higher temperatures where alloying elements begin to redistribute. In RT magnetic measurements, on the other hand, cementite with a low alloy content is initially ferromagnetic and its gradual enrichment by alloying elements such as Cr and Mn can be readily confirmed by the associated decrease in magnetization.

Due to the availability of the data regarding the influence of common alloying elements such as those in the ternary alloys studied in the present work on the magnetization of iron and cementite, dynamic microstructural changes during reheating of quenched ternary Fe-M-C steels (M denoting substitutional alloying elements) can be readily studied by the proposed magnetic method. The applicability of the method to the study of tempering reactions in engineering steels containing multiple substitutional alloying elements depends on the availability of the coefficients expressing their influence on the magnetization of ferrite and cementite. Due to the rareness of such data,[42] a first approximation would be to treat the effect of coexisting alloying elements as additive. Alternatively, such data may be obtained from theoretical calculations.[43,44]

IV. CONCLUSIONS

Tempering reactions in ternary Fe-2M-0.7C steels (M = Cr, Ni, Mn, Mo, and Si) were studied by correlative dilatometry and magnetic measurements at room temperature. Differences in the magnitude of demagnetization in the temperature range associated with the tempering stage I contraction indicated differences in the extent of transition carbides formation in the presence of different alloying elements; based on the magnitude of demagnetization, the Mn- and Si-added steels exhibited the highest and lowest fractions of transition carbides, respectively. After tempering at 673 K (400 °C), the rule of mixtures was used to calculate the magnetization of paraequilibrium cementite. In contrast to Mn, Cr, and Mo which decreased the magnetization of cementite, Ni raised it. In the presence of Si, the decomposition of retained austenite and cementite formation were shifted to higher temperatures. Subsequent to the formation of cementite, alloying elements were redistributed between martensite and cementite. The enrichment of cementite with Mn and Cr and the gradual decrease in the RT magnetization of cementite was associated with a decrease in the total magnetization which became noticeable at temperatures above 723 K (450 °C). In the Mo-added steel, on the other hand, the magnetization slightly increased implying the formation of ferromagnetic Mo-rich carbides. For the Ni- and Si-added steels, the magnetization remained almost constant

subsequent to the cementite formation indicating minimal redistribution of Ni and Si.

ACKNOWLEDGMENTS

The support of technical staff at the Institute of Iron and Steel Technology of TU Bergakademie Freiberg is gratefully acknowledged. G. Luan would like to thank the support of China Scholarship Council.

REFERENCES

1. M.K. Miller, P.A. Beaven, and G.D.W. Smith: *Metall. Trans. A*, 1981, vol. 12, pp. 1197–204.
2. S.J. Barnard, G.D.W. Smith, M. Sarikaya, and G. Thomas: *Scr. Metall.*, 1981, vol. 15, pp. 387–92.
3. C. Lerchbacher, S. Zinner, and H. Leitner: *Micron*, 2012, vol. 43, pp. 818–26.
4. K.A. Taylor and M. Cohen: *Prog. Mater. Sci.*, 1992, vol. 36, pp. 151–272.
5. Y. Ohmori and I. Tamura: *Metall. Trans. A*, 1992, vol. 23, pp. 2737–51.
6. S. Nagakura, Y. Hirotsu, M. Kusunoki, T. Suzuki, and Y. Nakamura: *Metall. Mater. Trans. A*, 1983, vol. 14A, pp. 1025–31.
7. G.R. Speich and W.C. Leslie: *Metall. Trans.*, 1972, vol. 3, pp. 1043–54.
8. C.B. Ma, T. Ando, D.L. Williamson, and G. Krauss: *Metall. Trans. A*, 1981, vol. 14, pp. 1033–45.
9. W. Crafts and J.L. Lamont: *AIME Tech. Publ.*, 1948, pp. 1–42.
10. T. Waterschoot, K. Verbeken, and B.C. De Cooman: *ISIJ Int.*, 2006, vol. 46, pp. 138–46.
11. Minsu. Jung, Seok.-Jae. Lee, and Young.-Kook. Lee: *Metall. Mater. Trans. A*, 2009, vol. 40A, pp. 551–59.
12. L. Cheng C.M. Brakman B.M. Korevaar E.J. Mittemeijer : *Metall. Trans. A*, 1988, vol. 19, pp. 2415–26.
13. L. Cheng E.J. Mittemeijer : *Metall. Trans. A*, 1990, vol. 21, pp. 13–26.
14. J.-G. Jung, M. Jung, S. Kang, and Y.-K. Lee: *J. Mater. Sci.*, 2013, vol. 49, pp. 2204–12.
15. M. Preciado and M. Pellizzari: *J. Mater. Sci.*, 2014, vol. 49, pp. 8183–91.
16. S. Primig and H. Leitner: *Thermochim. Acta*, 2011, vol. 526, pp. 111–17.
17. V.G. Gavriljuk: *Mater. Sci. Eng. A*, 2003, vol. 345, pp. 81–9.
18. Ph. Dünner and S. Müller: *Acta Metall.*, 1965, vol. 13, pp. 25–36.
19. H.S. Yang and H.K.D.H. Bhadeshia: *Mater. Sci. Technol.*, 2007, vol. 23, pp. 556–60.
20. J. Crangle and G.M. Goodman: *Proc. R. Soc. Lond. Ser. Math. Phys. Sci.*, 1971, vol. 321, pp. 477–91.
21. A.T. Aldred: *Phys. Rev. B*, 1976, vol. 14, pp. 219–27.
22. H. Yamauchi, H. Watanabe, Y. Suzuki, and H. Saito: *J. Phys. Soc. Jpn.*, 1974, vol. 36, pp. 971–74.
23. D. Parsons, W. Sucksmith, and J.E. Thompson: *Philos. Mag.*, 1958, vol. 3, pp. 1174–84.
24. J. Crangle and G.C. Hallam: *Proc. R. Soc. Lond. Math. Phys. Eng. Sci.*, 1963, vol. 272, pp. 119–32.
25. A.T. Aldred: *J. Phys. C Solid State Phys.*, 1968, vol. 1, p. 244.
26. J. Mola and B.C. De Cooman: *Metall. Mater. Trans. A*, 2013, vol. 44A, pp. 946–67.
27. R. Rahimi, H. Biermann, J. Mola, and R. Ritzenhoff: in *HNS 2014*, Hamburg, Germany, 2014, pp. 182–90.
28. R.M. Horn and R.O. Ritchie: *Metall. Trans. A*, 1978, vol. 9, pp. 1039–53.
29. L.J.E. Hofer and E.M. Cohn: *J. Am. Chem. Soc.*, 1959, vol. 81, pp. 1576–82.
30. K.O. Findley, J. Hidalgo, R.M. Huizenga, and M.J. Santofimia: *Mater. Des.*, 2017, vol. 117, pp. 248–56.
31. C. Zhu, X.Y. Xiong, A. Cerezo, R. Hardwicke, G. Krauss, and G.D.W. Smith: *Ultramicroscopy*, 2007, vol. 107, pp. 808–12.
32. A.J. Clarke, M.K. Miller, R.D. Field, D.R. Coughlin, P.J. Gibbs, K.D. Clarke, D.J. Alexander, K.A. Powers, P.A. Papin, and G. Krauss: *Acta Mater.*, 2014, vol. 77, pp. 17–27.
33. J. Akré, F. Danoix, H. Leitner, and P. Auger: *Ultramicroscopy*, 2009, vol. 109, pp. 518–23.
34. Akio. Kagawa and Taira. Okamoto: *Trans. Jpn. Inst. Met.*, 1979, vol. 20, pp. 659–66.
35. G.P. Huffman, P.R. Errington, and R.M. Fisher: *Phys. Status Solidi B*, 1967, vol. 22, pp. 473–81.
36. T. Shigematsu: *J. Phys. Soc. Jpn.*, 1974, vol. 37, pp. 940–45.
37. E.J. Seo, L. Cho, Y. Estrin, and B.C. De Cooman : *Acta Mater.*, 2016, vol. 113, pp. 124–39.
38. W. Pepperhoff and M. Acet: *Constitution and Magnetism of Iron and Its Alloys*, 1st ed., Springer, Berlin, 2001.
39. B.A. Apaev: *Magnetic Phase Analysis of Alloys*, Moscow Steel, Moscow, 1976.
40. T.P. Hou, Y. Li, Y.D. Zhang, and K.M. Wu: *Metall. Mater. Trans. A*, 2014, vol. 45A, pp. 2553–61.
41. Y.J. Li, P. Choi, S. Goto, C. Borchers, D. Raabe, and R. Kirchheim: *Acta Mater.*, 2012, vol. 60, pp. 4005–16.
42. I. Jacobs: *IEEE Trans. Magn.*, 1985, vol. 21, pp. 1306–09.
43. G. Rahman, I.G. Kim H.K.D.H. Bhadeshia, and A.J. Freeman: *Phys. Rev. B*, 2010, vol. 81, p. 184423.
44. M. Onoue, G. Trimarchi, A.J. Freeman, V. Popescu, and M.R. Matsen: *J. Appl. Phys.*, 2015, vol. 117, p. 043912.